Dalton Trans

ARTICLE

Received 00th January 20xx,

Accepted 00th January 20xx

DOI: 10.1039/x0xx00000x

www.rsc.org/

Modifying the Donor Properties of *Tris*(pyridyl)aluminates in Lanthanide (II) Sandwich Compounds

Raúl García-Rodríguez,[a*] Sara Kopf [b] and Dominic S. Wright [b]

The coordination ability of *tris*(pyridyl)aluminates can be modified by the steric and electronic character of substituents at the 6-positions of their pyridyl rings. Whereas $[EtAl(6\text{-Me-2-py})_3]^-$ (**1**) coordinates strongly to lanthanide (II) ions [Eu(II) and Yb(II)], $[EtAl(6\text{-Br-2-py})_3]^-$ (**2**) forms much weaker complexes, and $[EtAl(6\text{-}CF_3\text{-2-py})_3]^-$ does not coordinate at all. The modification of the donor ability of these ligands is investigated by solid-state studies of the Ln(II) sandwich compounds and by competitive coordination studies in solution.

1. Introduction

The coordination chemistry of neutral *tris*(2-pyridyl) ligands of the type $Y(2\text{-py})_3$ (Y = CR, COR, CH, N, P, P=O; 2-py = 2-pyridyl) (Figure 1a) has been thoroughly investigated in the past few decades[1] and has led to various applications in coordination, organometallic and bioinorganic chemistry.[2-4] Most recently, the first examples of tris-pyridyl ligands containing main group metallic bridgeheads have been investigated.[5-12] The introduction of a metallic bridgehead provides a simple approach to heterometallic complexes by the coordination of these ligands to other metals. *Tris*(2-pyridyl) aluminates are of particular interest as they are negatively charged rather than neutral (Figure 1b). As one of the few anionic members of the extensive family of *tris*-pyridyl ligands,[5,13] they exhibit strong affinities for metal cations and at the same time are isoelectronic with cyclopentadienide ligands (i.e., they are both formal 6e donors).[14-17]

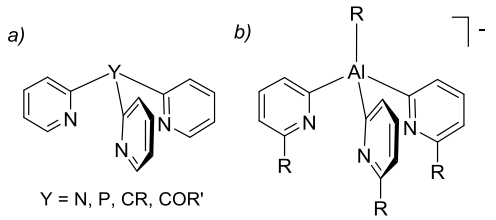

Figure 1 a) Neutral *tris*-(2-pyridyl) ligands containing non-metallic bridgehead atoms, b) 6-substituted *tris*-(2-pyridyl)-aluminates.

The framework of *tris*(2-pyridyl) aluminate ligands can be easily manipulated, allowing the control of their steric and donor character.[18,19] This can be achieved in two ways: a) by the selective replacement of one pyridine arm by an alkoxide group (giving a mixed O,N,N-donor functionality), and b) by the introduction of different substituents on the pyridyl rings. In particular, the introduction of substituents at the 6-position of the pyridine ring (i.e., adjacent to the nitrogen atom, Figure 1b) has a profound effect on the coordination properties of the aluminate, directly impacting the structure and stability of the metal complexes.[14] Sterically encumbered systems such as the $[EtAl(6\text{-Me-2-Py})_3]^-$ ligand (**1**) can kinetically stabilise metal ions in unusual oxidation states by shielding the metal cations. For instance, the introduction of 6-Me groups in the Sm(II) complex $[\{EtAl(6\text{-Me-2-py})_3\}_2Sm]$ results in significantly greater stabilization of the complex towards O_2 oxidation than its unsubstituted counterpart.[16]

Among the lanthanides, Eu and Yb are the most stable in the +2 oxidation state due to their half-filled f^7 and f^{14} electronic configurations. Their magnetic and optical properties as well as applications in catalysis mean that they are attractive targets for coordination studies.[20,21] Recently, sandwich complexes of Eu^{II} and Yb^{II} with *tris*(2-pyridyl) stannates as ligands have been prepared by reacting the lithium stannates with Cp^*_2Ln (Ln = Eu, Yb).[8] Notably, these complexes could not be prepared by the simple salt metathesis of Ln^{II} iodides and lithium stannate, which led only to the isolation of starting material.[11]

Here we report on the synthesis and properties of Eu^{II}- and Yb^{II}-sandwich complexes of 6-substituted *tris*(2-pyridyl) aluminates, and the influence of the steric and electronic properties of the *tris*(2-pyridyl) ligands on their coordination character and reactivity.

[a] *GIR MIOMeT-IU Cinquima-Química Inorgánica, Facultad de Ciencias, Campus Miguel, Delibes, Universidad de Valladolid 47011 Valladolid, Spain. E-mail: raul.garcia.rodriguez@uva.es.*

[b] *Chemistry Department. Cambridge University, Lensfield Road, Cambridge CB2 1EW (U.K.)*

Electronic Supplementary Information (ESI) avilable: NMR spectroscopic and X-ray characterisation. CCDC: 1587533 (**3**), 1587534 (**3·LiI**), 1587535 (**4**), 1587536 (**6**), 1587537 (**5**), 1587538 (**4·LiI**) DOI: 10.1039/x0xx00000x

2. Results and Discussion

2.1 Synthetic and Structural Studies

Synthetic and structural studies focused mainly on the two aluminate anions $[EtAl(6\text{-}Me\text{-}2\text{-}py)_3]^-$ (**1**) and $[EtAl(6\text{-}Br\text{-}2\text{-}py)_3]^-$ (**2**) (Scheme 1). As noted in the introduction, sterically-congested **1** is ideally suited for the stabilisation of lanthanide ions, which for the formation of Ln^{II} sandwich compounds usually requires sterically encumbered ligands (such as substituted cyclopentadienide ligands). The 2:1 stoichiometric reactions of the lithium salt of *tris*-$(6\text{-}Me\text{-}2\text{-}py)_3Al]^-$ (**1**) with LnI_2 (Ln = Eu, Yb) in thf at room temperature affords deep-orange or purple solutions (respectively) after 24 h, indicative of lanthanide complexation (Scheme 1a).

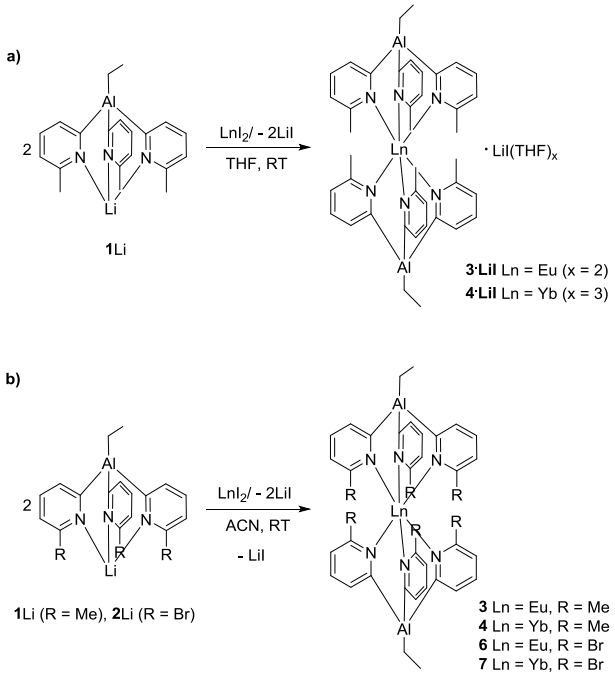

Scheme 1 Preparation of *tris*-pyridyl aluminate lanthanide sandwich complexes a) in thf as $Li(thf)_x$ adducts, and b) in acetonitrile as pure complexes in the absence of LiI.

Concentration of the solutions and storage at -15 °C gives orange and black crystals of $[EtAl(6\text{-}Me\text{-}2\text{-}py)_3]_2Ln\{LiI{\cdot}thf_x\}$ [Ln = Eu, **3**(LiI); Ln = Yb, **4**(LiI)], respectively. ^{7}Li and ^{1}H NMR spectroscopy and elemental analysis indicate the presence of thf-solvated LiI in the isolated crystalline samples. The Eu compound **3**(LiI) is isolated in modest yield (36 %), while the Yb complex **4**(LiI) is only obtained in very low yield (*ca.* 4 %). Single-crystal X-ray crystallography confirms that the sandwich compounds $[\{EtAl(6\text{-}Me\text{-}2\text{-}py)_3\}_2Ln]$ (Ln = Eu, Yb) co-crystallise with thf-solvated LiI in both cases. In the case of **3**(LiI) there is one dimeric $[(thf)_2Li(\mu\text{-}I)]_2$ unit per unit of **3** in the crystal lattice, while the solid-state structure of **4**(LiI) contains two *tris*-solvated $(thf)_3LiI$ units for each molecule of **4** (see ESI, Fig S32). Molecules of **3** and **4** feature six-coordinate, distorted-octahedral lanthanide metal ions with the N–Ln–N angles being approximately 90° (Figure 2a). The Ln-N bond lengths in **4** [range 2.564(4)-2.611(4) Å] are about 0.1 Å shorter than in **3** [range 2.689(3)-2.696(3) Å]. For comparison, the Sm-N bond lengths in the previously reported isostructural sandwich compound $[\{EtAl(6\text{-}Me\text{-}2\text{-}py)_3\}]_2Sm^{II}]$ are in the range 2.666(3)-2.721(3) Å.[16] The trend in the N-Ln bond lengths in all of these species correlates well with the ionic radii of the lanthanide ions: Sm^{2+} (1.36 Å) ≈ Eu^{2+} (1.31 Å) > Yb^{2+} (1.16 Å).[22] As seen in the space-filling view of molecules of **3** and **4**, the 6-methyl groups interdigitate, providing steric shielding of the lanthanide centres (Figure 2b). This effect appears to be responsible for the stabilisation of the previously reported Sm^{2+} complex against O_2 oxidation.[16]

Owing to the similar solubility of LiI and the sandwich compounds in thf and toluene, fractional crystallisation from these solvents did not afford the pure lanthanide complexes, free of LiI. However, switching the reaction solvent from thf/toluene to acetonitrile facilitates purification dramatically. The 2:1 stoichiometric reactions of aluminate **1** and LnI_2 (Ln = Eu, Yb) at room temperature in acetonitrile results in the formation of the sandwich complexes $[\{EtAl(6\text{-}Me\text{-}2\text{-}py)_3\}_2Ln]$ (Ln = Eu (**3**), Yb (**4**)), which cleanly precipitate from the reaction media (Scheme 1b). Under these conditions, **3** and **4** are obtained *without* contamination by LiI and in higher yields (69 % for **3**, 48 % for **4**), as orange (**3**) and deep purple (**4**) microcrystalline solids that were analytically and spectroscopically pure. In particular, no $LiI(thf)_x$ was detected by ^{7}Li or ^{1}H NMR. Single-crystal X-ray analysis of **3** and **4** confirmed that the structures of both are identical (within the crystallographic errors) to the sandwich molecules present in **3**(LiI) and **4**(LiI), but with no thf-solvated LiI units being present (see Table S2 in the ESI).

It is interesting that despite the relatively large ionicity of the Al-C bond, the aluminate anion **1** is stable in acetonitrile with no deprotonation or insertion reactions being observed after 24 h at 25 °C. Compound **3** can also be obtained by the 2:1 reaction of **1**Li and $Eu(OTf)_3$ in acetonitrile (in 12 % yield). This reaction presumably involves reduction of Eu(III) to Eu(II) and the formation of 6,6′-dimethyl-2,2′-bipyridine (Scheme 2). This is similar to the reduction of $EuCl_3$ in the presence of NaCp* to give $Eu(Cp^*)_2$ (presumably with concomitant formation of Cp*-Cp*),[23,24] and the oxidative coupling of the plumbate $[(6\text{-}^t\text{BuO-Py})_3Pb]^-$ to Pb-Pb bonded $[(6\text{-}^t\text{BuO-Py})_3PbPb(6\text{-}^t\text{BuO-Py})_3]$.[25]

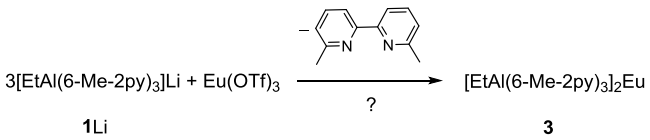

Scheme 2 Formation of complex **3** from the reduction of $Eu(OTf)_3$.

Although NMR spectroscopic studies of the Eu^{II} complex **3** were precluded by its paramagnetic nature, the diamagnetic f^{14} Yb^{II} complex **4** was amenable to NMR spectroscopy. A detailed ^{1}H NMR spectroscopic study in thf-d_8 allowed unambiguous assignment of the NMR signals, with the help of additional 2D NMR experiments (see ESI). The room-

temperature ^{1}H NMR spectrum shows one set of pyridyl resonances and the characteristic set of signals for the ethyl group. Interestingly, coordination to Yb^{2+} results in a significant upfield shift of the 6-Me group by 1.1 ppm whereas the ethyl resonances are downfield (*ca.* 0.2 ppm) compared to **1**Li. The NMR studies suggest that the sandwich arrangement of **4** is retained in solution.

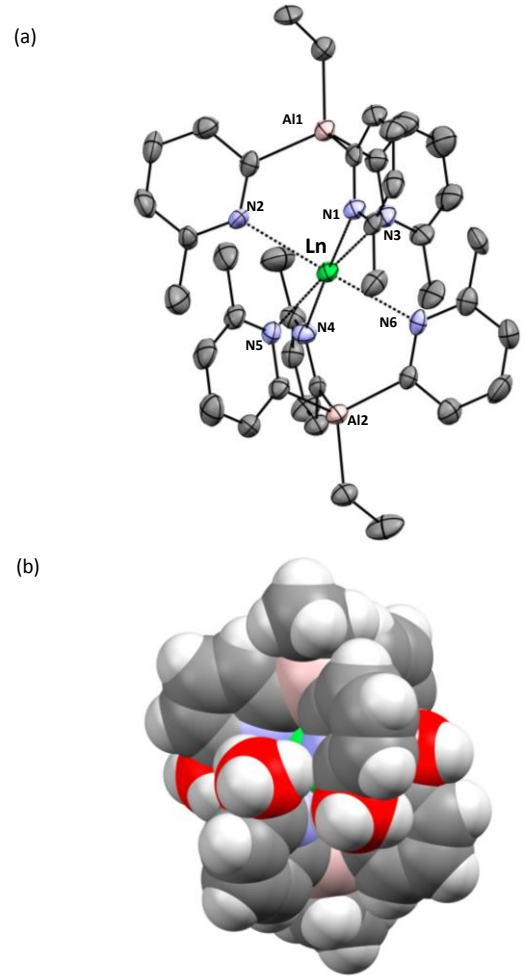

Figure 2 a) The common structure of the sandwich compounds **3** and **4** (the picture is drawn from the data for **4**). Thermal ellipsoids are drawn at the 40% probability level. Selected bond lengths (Å) and angles (°): for **3**, C_{Et}–Al 1.988(4), C_{py}–Al range 2.014(4)-2.036(4), Al···Ln 3.564(1), Eu-N range 2.689(3)-2.696(3), C_{py}–Al–C_{py} range 104.6(2)-113.4(1), Al–C_{py}–N range 121.4(4)-123.8(3), N–Eu–N range 88.5(1)-91.51(9); for **4**, C_{Et}–Al 1.994(5), C_{py}–Al range 2.007(5)-2.023(5), Al···Yb 3.459(1), Yb-N range 2.564(4)-2.611(4), C_{py}–Al–C_{py} range 105.6(2)-112.4(2), Al–C_{py}–N range 120.3(2)-123.9(3), N–Yb–N range 85.6(1)-94.4(1). b) Space-filling representation of molecules of **3** and **4** with 6-methyl groups highlighted in red. Selected bond lengths and angles for the LiI-free compounds **3** and **4** are presented in Table S2 in the ESI.

The 2:1 reaction of **1**Li with YbI_2 (forming diamagnetic Yb^{II} compound **4**) was followed by *in situ* ^{1}H NMR spectroscopy in thf-d_8. Mixing for 2.5 h leads to the formation of the half-sandwich complex [EtAl(6-Me-2py)$_3$YbI(thf)$_2$] (**5**) as an intermediate. This is completely converted into the sandwich compound **4** after heating to 50 °C for 24 h. The half-sandwich **5** can be prepared in good yield (49%) selectively by the 1 : 1 reaction of **1**Li with YbI_2 in thf.

The composition of **5** was confirmed by single-crystal X-ray crystallography of the thf solvate **5**·thf, the molecular structure of which is shown in Figure 3. The central Yb^{II} atom is in a distorted octahedral environment, coordinated to the N-atoms of the pyridyl rings of the aluminate ligand **1**, two molecules of thf and one iodine atom. The ethyl group and one pyridine ring lie on a mirror plane that passes through the Yb, I and Al atoms. The Yb-N bond lengths in **5** are slightly shorter than in the sandwich compound **4** [2.505(8)-2.534(5) Å *vs.* 2.564(4)-2.611(4) Å]. No examples of monomeric half-sandwich compounds of the Cp-family of the type ($CpLn^{II}X$) (X=halogen) have been structurally characterised previously, although a few similar half-sandwich arrangements have been reported for *tris*-pyrazolyl-borates complexes.[26]

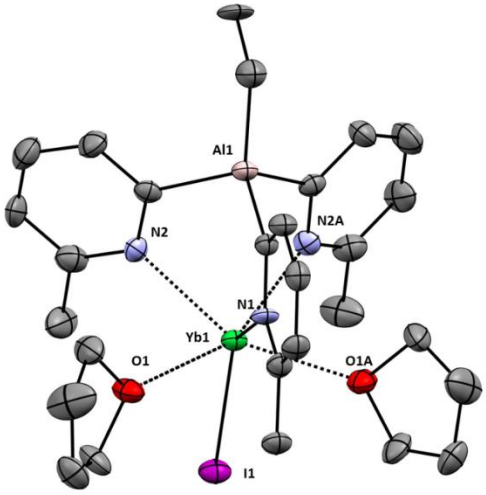

Figure 3 Structure of the half-sandwich compound **5**. The lattice thf molecule and H-atoms have been omitted for clarity. Thermal ellipsoids are drawn at the 40% probability level. Selected bond lengths (Å) and angles (°): C_{Et}–Al 1.98(1), C_{py}–Al range 2.022(7)-2.035(5), Al···Yb 3.448(3), Yb-I 3.1020(8), Yb-O 2.535(5), Yb-N range 2.505(8)-2.534(5), C_{py}–Al–C_{py} range 104.3(4)-108.7(2), Al–C_{py}–N range 119.1(6)-121.7(5), N–Yb–N range 82.0(3)-98.7(2).

We next investigated the complexation of Eu^{II} and Yb^{II} using other aluminates [EtAl(6-R-2-py)$_3$] bearing electron-withdrawing groups (R = -CF_3, -Br). Reactions of [EtAl(6-Br-2-py)$_3$]Li (**2**Li) with EuI_2 and YbI_2 in acetonitrile at room temperature result in the precipitation of the sandwich complexes [{EtAl(6-Br-2-py)$_3$]}$_2$Eu] (**6**) and [{EtAl(6-Br-2-py)$_3$]}$_2$Yb] (**7**) as orange and dark ruby solids after 1.5 h and 3.5 h, respectively (Scheme 1b). The compounds were isolated in moderate yields (56% and 43% for **6** and **7**, respectively) and their purity was established by elemental analysis. The absence of LiI in **7** was confirmed by ^{7}Li NMR and elemental analysis. The NMR spectroscopic data (^{1}H, ^{13}C, and ^{27}Al, see ESI) is consistent with retention of the sandwich arrangement in solution. The room-temperature ^{1}H NMR spectrum shows a set of signals for the 6-Br-2-py group as well as the characteristic set of signals for the ethyl group. As observed in the case of analogous Yb^{II} complex **4**, the ethyl group of the aluminate ligand of **7** is downfield (*ca.* 0.4 ppm) with respect to **2**Li. The three pyridyl protons of the 6-Br-2-py group in **7** are

downfield in comparison to those of the 6-Me-2-py group in **4** by up to 0.4ppm for H^5 (i.e. the proton adjacent to the substituent), reflecting the electron withdrawing ability of the Br atom.

In contrast to the *in situ* ^{1}H NMR study of the 2 : 1 reaction of **1**Li with YbI_2 in thf, which shows quantitative formation of the sandwich compound **4** (see above), an *in situ* ^{1}H NMR study of the reaction of **2**Li with YbI_2 (2:1) in thf-d_8 shows that only a small amount (ca. 5%) of the sandwich complex **7** is generated even after 24 h at 50 ^{o}C. Prolonged heating at 50 ^{o}C (48 h) only resulted in the formation of additional unknown species in low concentration, which could not be identified, with unreactive **2**Li being the major species present (ca. 90%). Furthermore, a 2 : 1 mixture of EtAl(6-CF_3-2-py)$_3$Li and EuI_2 in acetonitrile showed no sign of reaction after several days at room temperature, or after prolonged heating of the reaction mixture (with no diagnostic colour change being observed). The poor coordination ability of the [EtAl(6-CF_3-2-py)$_3$]$^-$ anion appears to be due to the large steric bulk and strongly electron-withdrawing nature of the CF_3 group, having the combined effect of retarding metal coordination and reducing the electron-donating ability of the pyridyl N-atoms. This lack of coordination ability was noted by us earlier in respect to Fe(II).[18]

The solid-state structure of **6** is closely related to those of **3** and **4**, revealing a six-coordinate, distorted-octahedral Eu^{2+} ion (Figure 4). An interesting observation is that of the significantly longer Eu-N bond lengths in **6** compared to the 6-Me substituted Eu^{II} sandwich **3** [2.689(3)-2.696(3) Å *vs.* 2.754(4)-2.795(4) Å]. Since the van der Waals radius of Br is smaller than that of a methyl group (*ca.* 1.85 Å versus *ca.* 2.23 Å)[27] this must be largely a reflection of the lower donor ability of **2** compared to **1**, resulting from the electron withdrawing effect of the Br atoms on the available N-electron density. The poorer ligating ability of **2** is confirmed by in-depth NMR studies of the ligand-exchange reactions of ytterbium complexes **4** and **7**, described in the next section of this paper. This shows that although **2** has diminished ligand ability compared to **1**, it is still able to form Yb complexes, in contrast to the [EtAl(6-CF_3-2-py)$_3$]$^-$ anion. The labile nature of the resultant ytterbium complexes can be exploited in the formation of heteroleptic complexes, as shown in the next section.

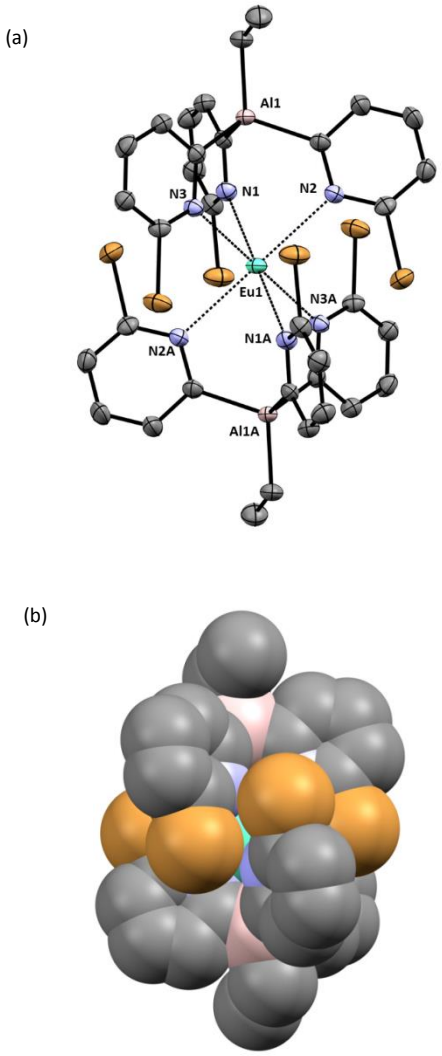

Figure 4 (a) Structure of the sandwich compound **6** (in the thf solvate **6**·2thf). Thermal ellipsoids are drawn at the 40% probability level. H-atoms and solvate thf molecules in the lattice have been omitted for clarity. Selected bond lengths (Å) and angles (^{o}): C_{Et}–Al 1.994(5), C_{py}–Al range 2.010(5)-2.019(6), Al···Eu 3.807(6), Ln-N range 2.754(4)-2.795(4), C_{py}–Al–C_{py} range 105.8(2)-111.5(3), Al–C_{py}–N range 120.3(4)-124.0(4), N–Eu–N range 84.1(1)-95.9(1). (b) Space-filling representation (the Br atoms are coloured orange).

2.2 Ligand-Exchange Reactions

An intriguing observation noted in the *in situ* NMR spectroscopic studies in the previous section was that the Yb^{II} sandwich compound **4** (containing 6-Me ligand **1**) is readily obtained in thf. In contrast, the NMR studies reveal that the Yb^{II} sandwich compound **7** (containing 6-Br ligand **2**) is only observed in trace amounts in thf even after prolonged heating at 50 ^{o}C. This is explained by further NMR spectroscopic studies of the behaviour of **4** and **7** in the presence of LiI.

Addition of excess of anhydrous LiI (*ca*. 6 equivalents) to a solution of the sandwich compound **4** in thf-d_8 at room temperature does not result in any change in the ^{1}H NMR spectrum even after 7 days at room temperature. Compound **4** is also stable upon addition of 1.5 equivalents of YbI_2, with no

formation of the half-sandwich compound **5** being observed. In contrast, addition of *ca.* 0.2 equivalents of LiI to **7** at room temperature results in the formation of **2**Li and a second species which is assigned to the half-sandwich compound **8** (Scheme 3 and Figure 5). Further addition of LiI results in the progressive disappearance of **7** and the concomitant formation of **2**Li and **8**, until almost no sandwich complex **7** is observed in the ^{1}H NMR spectrum after the addition of *ca.* 1 equivalent of LiI. An excess of LiI (*ca.* 6 equivalents) results in an immediate colour change from dark ruby to colourless, along with the complete disappearance of the resonances for **7** and **8** and the presence of **2**Li as the only species in the ^{1}H NMR spectrum (Fig. 5e).

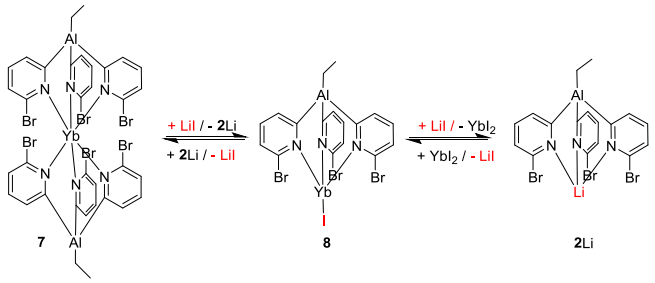

Scheme 3 Reaction of the Yb^{II} sandwich **7** with LiI.

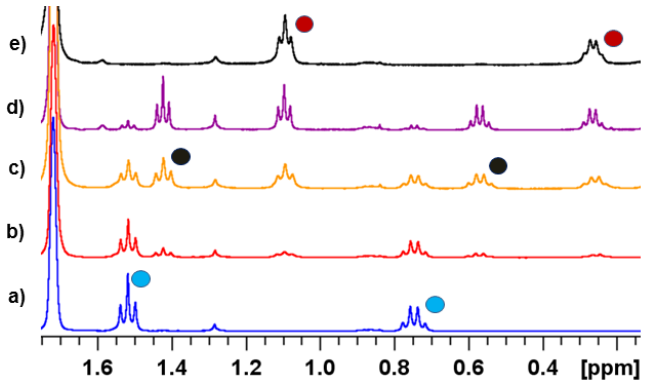

Figure 5 ^{1}H NMR spectra (ethyl region) of a thf-d$_8$ solution of (a) sandwich complex **7**, (b) + *ca.* 0.2 equivalents of LiI, (c) + 0.5 equivalents of LiI, (d) + 1 equivalent of LiI, and (e) an excess of LiI. Colour code: **7** (blue circles), **8** (black circles), **2**Li (red circles).

In order to explore the relative coordination ability of the aluminates **1** and **2** directly, we also studied the behaviour of **4** and **7** in the presence of the lithium salts **1**Li and **2**Li. The addition of 0.2–2.2 equivalents of **1**Li to a solution of **4** in thf-d$_8$ at room temperature resulted in sharp signals in the ^{1}H NMR spectrum at the expected chemical shifts for the two independent species. No dynamic processes were detected by ^{1}H-^{1}H NOESY or ^{1}H-^{1}H ROESY (see ESI). This showed that both species coexist independently in solution and that no interchange of the aluminate **1** occurs in solution between the lithium salt and the ytterbium sandwich on the NMR timescale. However, ^{1}H-^{1}H NOESY and ^{1}H-^{1}H ROESY experiments indicate the presence of a dynamic equilibrium between the bromo- counterparts **7** and **2** when **2**Li is added to a solution of **7** in thf-d$_8$. As seen in Figure 6a, the two sets of signals in the ethyl group region for **2** and **7** undergo chemical exchange, consistent with transfer of the *tris*-pyridyl aluminate anion between the Yb^{II} and lithium centres. If a small amount of LiI is added to the mixture of **2**Li and **7**, the ^{1}H-^{1}H NOESY and ^{1}H-^{1}H ROESY experiments also show that there is a dynamic-exchange equilibrium between **2**, **7** and the half-sandwich **8** (Figure 6b). The potential for these exchange reactions to occur *via* an associative mechanism is supported by the reported formation of Ln(Cp)$_3^-$ complexes by the addition of Cp$^-$ to LnCp$_2$.[22-24] However, due to poor solubility of **7** in thf, further kinetic studies to confirm this could not be conducted.

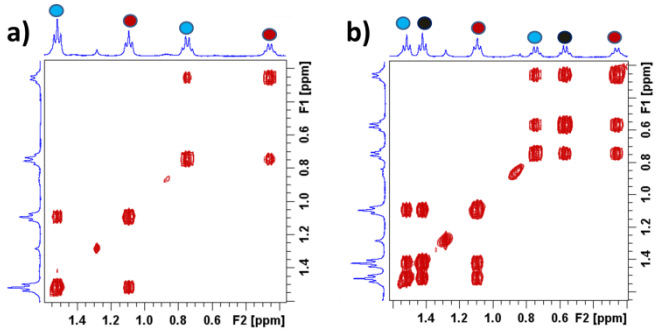

Figure 6 ^{1}H-^{1}H NOESY spectra (ethyl region) in thf-d$_8$ of a mixture of (a) **2**Li and **7** and (b) a mixture of **2**, **7** and **8**. Colour code: **7** (blue circles), **8** (black circles), **2**Li (red circles). The chemical exchange observed in the NOESY spectra was also observed in the ^{1}H-^{1}H ROESY experiments, thus confirming the chemical exchange.

Finally, the interaction of 2.2 equivalents of **1**Li with **7** was monitored by ^{1}H and ^{7}Li NMR spectroscopy at room temperature in thf-d$_8$. Within 36 h the signals for **7** disappear and are replaced by those of [EtAl(6-Me-2-py)$_3$]$_2$Yb (**4**) and **2**Li. This process involves the heteroleptic Yb(II) sandwich compound [{EtAl(6-Me-2-py)$_3$}{EtAl(6-Br-2-py)$_3$}Yb] (**9**) as an intermediate (Scheme 4). Although attempts to isolate **9** were unsuccessful, it was characterized by *in situ* solution NMR spectroscopy in the reaction of **7** with a sub-stoichiometric amount of **1**Li (0.5-1 equivalents), giving **2**Li and **9** in a 1:1 ratio (Scheme 4 and ESI). Further support for the formation of **9** in this case is provided by the addition of LiI to this mixture, which, as expected on the basis of the studies described previously, results in the half-sandwich **5**.

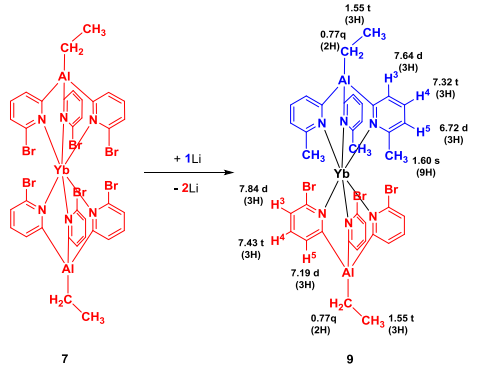

Scheme 4 Assignment of the ^{1}H NMR spectrum of the heteroleptic complex **9** from the *in situ* ^{1}H NMR spectrum and additional 2D experiments. The ethyl

groups of the two aluminates overlap, giving rise to a pseudo quartet and a multiplet instead of the expected triplet and quartet.

Also, as expected from the above studies, attempts to prepare complex **9** by reacting sandwich complex **3** or half sandwich complex **5** with **2**Li failed. This highlights that the understanding of the different coordination behaviour of tris(pyridyl)aluminates is crucial for the rational design of heteroleptic sandwich complexes.

Conclusions

This study has shown that 6-pyridyl-substituted *tris*-pyridyl aluminates can be used to prepare relatively stable sandwich-like coordination compounds with divalent metal lanthanide ions. The substituent at the 6-position clearly has a marked steric and electronic impact on the coordination ability of these ligands, with the sterically-demanding, electron withdrawing CF_3-substituents being unable to coordinate to lanthanide ions, Br-substituents resulting in weak coordination and Me-substituents resulting in the strongest coordination. This study also establishes the basis for the rational synthesis of heteroleptic sandwiches of this type.

Acknowledgements

We thank the Spanish MINECO-AEI and the European Union (ESF) for a Ramon y Cajal contract (RG-R, RYC-2015–19035) and the EU (Erasmus+ grant for SK). We also thank Dr A. D. Bond for collecting X-ray data on compound **6**.

Experimental

All syntheses were carried out on a vacuum-line under nitrogen atmosphere using dry solvents. Products were isolated and handled in a nitrogen-filled glove box (Saffron type α). Toluene, thf and *n*-hexane were dried under nitrogen over sodium or sodium/benzophenone, respectively, whereas acetonitrile was dried over calcium hydride. Anhydrous EuI_2 and YbI_2 (≥99.9%) were purchased from Aldrich in ampules. The ampules were opened inside a N_2-filled glovebox and were used without any further purification. [EtAl(6-Me-2-py)$_3$Li] (**1**Li) and [EtAl(6-Br-2-py)$_3$Li] (**2**Li) were prepared according to previously published procedures.[18] ^{1}H and ^{7}Li NMR spectra were recorded on a Bruker Advance 400 QNP or a Bruker Advance 500 MHz Cryo spectrometer. ^{13}C and ^{27}Al spectra were recorded on a Bruker Advance 500 MHz Cryo spectrometer. All spectra were recorded in dry thf-d_8 or dry toluene-d_8. The unambiguous assignment of NMR resonances was accomplished by additional 2D experiments (^{1}H-^{1}H COSY, ^{1}H-^{1}H NOESY, ^{1}H-^{1}H-ROESY, ^{1}H-^{13}C HMQC, ^{1}H-^{13}C-HMBC). Figure 7 shows the labelling scheme for NMR assignments. Elemental analysis was obtained on a Perkin Elmer 240 Elemental Analyser. Elemental analyses on all of the compounds were complicated by their air- and moisture-sensitivity and potentially by the formation of metal carbides during their combustion. The latter is indicated by the experimentally determined C contents obtained for compounds **4, 5, 6** and **7**, which were consistently ca. 1-2 % lower than the calculated values over several analyses. In the case of **3**(LiI) and **4**(LiI) elemental analysis was hampered by the rapid loss of thf desolvated from samples during isolation .The values reported here are the best obtained over several analyses on a single sample.

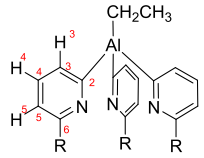

Figure 7. Atom labelling used in the NMR studies.

X-ray Crystallographic Studies. Data were collected for **3**, **4**LiI and **5** on a Bruker D8 QUEST Photon-100 diffractometer with an Incoatec IμS Cu microfocus source; for **4** on a Bruker SMART X2S diffractometer with a monochromatic MoKα microfocus source; and for **6** and **3Li** on a Nonius KappaCCD diffractometer with graphite-monochromated MoKα radiation. The temperature was held between 180 and 220 K using an Oxford Cryosystems N_2 cryostat. Crystals were mounted directly from solution using perfluorohydrocarbon oil to prevent atmospheric oxidation, hydrolysis and solvent loss. [28] Further details can be found in the ESI, including details of the data collection and refinement (Table S1) and selected bond lengths and angles (Table S2) of the compounds. CCDC: 1587533 (**3**), 1587534 (**3**·LiI), 1587535 (**4**), 1587536 (**6**), 1587537 (**5**), 1587538 (**4**·LiI).

Synthesis of compounds 1–7:

*Synthesis of [EtAl(6-Me-2-py)$_3$]$_2$Eu·[(thf)$_2$Li(μ-I)]$_2$ [**3**(LiI)]:* A solution of EuI_2 (90 mg, 0.222 mmol) in thf (8 mL) was added dropwise to a solution of [EtAl(6-Me-2-py)$_3$Li] (150 mg, 0.442 mmol) in toluene (10 mL) at room temperature. The yellow solution was stirred at room temperature (22 h) and slowly turned orange. The resulting orange solution was concentrated until the precipitation of an orange solid was observed. The solid was redissolved by gently heating the solution. Crystalline red needles were obtained by layering the saturated solution with *n*-hexane and storing the sample at -15 °C for 24 h. Total isolated crystalline yield: 110 mg, 0.0801 mmol, 36 %. Characterisation by NMR techniques was significantly hampered by the paramagnetism of the compound. Thus, ^{1}H and ^{13}C spectra could not be obtained. ^{7}Li NMR (+25 °C, d_8-thf, 194 MHz), δ = 0.73 (s) ppm. Elemental analysis, calcd for **3**·(LiI)$_2$·(thf)$_2$, C 49.0 %, H 5.7 %, N 6.1 %; found: C 47.2 %, H 5.5 %, N 7.6 %. Elemental analysis was hampered by the rapid loss of thf desolvated from samples during isolation. This process results in loss of crystallinity and the extrusion of LiI, as confirmed by ^{7}Li NMR. This process ultimately produces heterogeneous samples containing **3** and LiI if samples are left under persistent vacuum.

*Synthesis of [EtAl(6-Me-2-py)$_3$]$_2$Yb·2(thf)$_3$LiI [**4**(LiI)]:* YbI_2 (94 mg, 0.220 mmol) and [EtAl(6-Me-2-py)$_3$Li] (150 mg, 0.442 mmol) were added to a Schlenk tube in a glove box. The Schlenk tube was transferred to a vacuum line and the solids were dissolved in thf (5 mL). The dark red solution was stirred for 24 h at room temperature. The resulting deep red solution was concentrated *in vacuo*. Black crystals were observed by layering the saturated solution with *n*-hexane and storing the solution at -15 °C for 20 h. Total isolated crystalline yield: *ca* 13 mg, 0.0084 mmol, 4 %. As found for **3**LiI, elemental analysis was hampered by the rapid loss of thf solvent from samples during isolation and satisfactory analysis could not be obtained for this complex. This process results in loss of crystallinity and the extrusion of LiI, as confirmed by ^{7}Li NMR. This process ultimately produces heterogeneous samples containing **3** and LiI if samples are left under persistent vacuum. However, the spectroscopic data on the complex is identical to that of unsolvated **4** (see below), apart from the presence of solvated LiI: ^{7}Li NMR (+25 °C, d_8 thf, 194 MHz), δ = 0.72 (s) ppm. ^{1}H NMR (+25 °C, d_8-thf, 400 MHz), δ = 3.62 (m,–CH_2–O, thf), 1.77 (m, –CH_2–, thf).

*Synthesis of [EtAl(6-Me-2-py)$_3$]$_2$Eu (**3**):* EuI_2 (180 mg, 0.444 mmol) and [EtAl(6-Me-2-py)$_3$Li] (300 mg, 0.884 mmol) were added to a Schlenk tube in a glovebox. The Schlenk tube was transferred to a vacuum line and the solids were dissolved in acetonitrile (10 mL). Within 5 min, the initially pale yellow suspension became orange and an orange precipitate began to form. The reaction mixture was stirred for 2 h at room temperature before the precipitate was isolated by filtration. The absence of LiI was confirmed by ^{7}Li NMR spectroscopy. Yield: 250 mg, 0.306 mmol, 69 %. Elemental analysis, calcd. for **3**, C 58.8 %, H 5.7 %, N 10.3 %; found: C 58.3 %, H 5.1 %, N 10.1 %. Red crystals suitable for X-ray analysis could be obtained by layering a saturated solution of **3** in thf with *n*-hexane and storing the sample at -15 °C for 20 h. Total isolated crystalline yield: 100 mg, 0.122 mmol, 27 %. Characterisation by NMR techniques was significantly hampered by the paramagnetism of the compound. Thus, ^{1}H and ^{13}C spectra could not be obtained.

*Synthesis of [EtAl(6-Me-2-py)$_3$]$_2$Yb (**4**):* YbI_2 (190 mg, 0.445 mmol) and [EtAl(6-Me-2-py)$_3$]Li (300 mg, 0.884 mmol) were added to a Schlenk flask in a glove box. The Schlenk tube was transferred to a vacuum line and the solids were dissolved in acetonitrile (8 mL). The resulting red suspension became maroon after 15 min and was stirred at room temperature for one hour and subsequently filtered to obtain a black precipitate. The absence of LiI was confirmed by ^{7}Li NMR spectroscopy. Yield: 180 mg, 0.215 mmol, 48 %. Elemental analysis, calcd. for **4**, C 57.3 %, H 5.5 %, N 10.0 %; found: C 55.3 %, H 5.1 %, N 10.5 %. Layering a saturated solution of **4** in thf with *n*-hexane afforded black crystals suitable for X-ray analysis. ^{1}H NMR (+25 °C, d_8-thf, 400 MHz), δ = 7.70 (d, J_{HH} = 6.4 Hz, 6 H, C(3)-H py), 7.38 (d, J_{HH} = 7.0 Hz, 6 H, C(4)-H py), 6.72 (d, J_{HH} = 7.1 Hz, 6 H, C(5)-H py), 1.55 (t, J_{HH} = 7.2 Hz, 6 H, Al-CH_2CH_3), 1.44 (s, 18 H, C(6) CH_3), 0.77 (q, J_{HH} = 7.6 Hz, 4 H, Al-CH_2) ppm. ^{13}C NMR (+25 °C, d_8-thf, 126 MHz): δ = 187.2 (br, C(2)), 158.74 (C(6)), 134.10 (C(4)), 131.61 (C(3)), 122.57 (C(5)), 22.76 (C(6)-CH_3), 10.70 (Al-CH_2CH_3), -0.39 br, (Al-CH_2) ppm. ^{27}Al-NMR (+25 °C, d_8-thf, 130 MHz): δ = 132 ppm (br, s).

*Synthesis of [EtAl(6-Me-2py)$_3$YbI(thf)$_2$·thf] (**5**):* YbI_2 (255 mg, 0.60 mmol) was combined with thf (10 mL) and the mixture was stirred for 10 min at room temperature and further sonicated for 2 min. After that a solution of [EtAl(6-Me-2-py)$_3$Li] (200 mg, 0.59 mmol) in thf (5 mL) was added dropwise. The mixture was stirred at room temperature for 4 h and subsequently filtered, giving a deep red solution that was concentrated under vacuum (*ca*. 8 mL). Slow diffusion of *n*-hexane at -15 °C afforded red crystals of **5**·thf that were suitable for X-ray studies. Yield: 230 mg, 0.278 mmol, 47 %. Elemental analysis, calcd. for **5**, C 43.3 %, H 5.1 %, N 5.4 %; found: C 42.6 %, H 5.1 %, N 5.3 %. Note: variable amounts of LiI were observed in samples (^{7}Li NMR) as white crystals that were separated manually. The values reported here are the best obtained over several analyses on a single sample and correspond to the unsolvated compound (i.e., no lattice thf). ^{1}H NMR (+25 °C, d_8-thf, 400 MHz), δ = 7.57 (d, J_{HH} = 7.2 Hz, 3 H, C(3)-H py), 7.38 (d, J_{HH} = 7.5 Hz, 3 H, C(4)-H py), 6.91 (d, J_{HH} = 7.7 Hz, 3 H, C(5)-H py), 3.62 (m, 8 H, –CH_2–O, thf), 2.77 (s, 9 H, C(6)–Me), 1.77 (m, 8 H, –CH_2–, thf), 1.40 (t, J_{HH} = 8.0 Hz, 3 H, Al-CH_2CH_3), 0.63 (q, J_{HH} = 8.0 Hz, 2 H, Al-CH_2) ppm. ^{13}C NMR (+25 °C, d_8-thf, 126 MHz): δ = 186.8 (br, C(2)), 157.90 (C(6)), 134.28 (C(4)), 131.51 (C(3)), 122.38 (C(5)), 68.23 (CH_2O, thf), 26.37 (–CH_2–, thf), 25.42 (C(6)-CH_3, signal overlapped with thf-d_8 signal. Detected through a ^{1}H-^{13}C HMQC experiment), 10.59 (Al-CH_2CH_3), -1.9 (br, Al-CH_2) ppm. ^{27}Al-NMR (+25 °C, d_8-thf, 130 MHz): δ = 129 ppm (br, s).

*Synthesis of [EtAl(6-Br-2-py)$_3$]$_2$Eu (**6**):* EuI_2 (90 mg, 0.222 mmol) and [EtAl(6-Br-2-py)$_3$Li] (235 mg, 0.440 mmol) were added to a Schlenk flask in a glovebox. The Schlenk tube was transferred to a vacuum line and the solids were dissolved in acetonitrile (4 mL). The resulting intense yellow suspension was stirred at room temperature for 75 min and subsequently filtered in order to isolate a yellow precipitate. Yield: 150 mg, 0.124 mmol, 56 %. Elemental analysis, calcd. for **6**, C 33.8 %, H 2.3 %, N 7.0 %, found: 33.1 %, 2.3 %, 7.1 %. Layering a saturated solution of **6** in THF with *n*-hexane afforded yellow crystals suitable for X-ray analysis of the thf solvate **6**·thf. Total isolated crystalline yield: 70 mg, 0.058 mmol, 26 %. Isolation under vacuum gave amorphous material which was found to contain no thf. The analytic results listed correspond to this material. Characterisation by NMR techniques was significantly hampered by the paramagnetism of the compound.

*Synthesis of [EtAl(6-Br-2-py)$_3$]$_2$Yb (**7**):* YbI_2 (190 mg, 0.445 mmol) and [EtAl(6-Br-2-py)$_3$Li] (470 mg, 0.880 mmol) were added to a Schlenk tube in a glovebox. The Schlenk tube was transferred to a vacuum line and the solids were dissolved in acetonitrile (4 mL). The initially red suspension became red-brown upon stirring at room temperature for 3.5 h. Filtration and washing with toluene afforded a ruby solid. Yield: 235 mg, 0.192 mmol, 43 %. Elemental analysis: calculated for **7**: C 33.3 %, H 2.3 %, N 6.9 %, found: C 32.9 %, H 2.4 %, N 6.8 %. The absence of LiI was confirmed by ^{7}Li NMR spectroscopy. ^{1}H-NMR (+25 °C, d_8-thf, 400 MHz), δ = 7.79 (d, J_{HH} = 7.0 Hz, 6 H, C(3)-H py), 7.38 (t, J_{HH} = 7.7 Hz, 6 H, C(4)-H py), 7.16 (d, J_{HH} = 7.8 Hz, 6 H, C(5)-H py), 1.52 (t, J_{HH} = 8.0 Hz, 6 H, Al-CH_2CH_3), 0.75 (q, J_{HH} = 7.9 Hz, 4 H, Al-CH_2) ppm. ^{13}C NMR (+25 °C, d_8-thf, 126 MHz), δ = 190.6 (br, C(2)), 144.71 (C(6)), 136.65 (C(4)), 133.21 (C(3)), 127.78 (C(5)), 10.47 (Al-CH_2CH_3), -0.60 (br, Al-CH_2) ppm. ^{27}Al-NMR (+25 °C, d_8-thf, 130 MHz): δ = 133 ppm (br, s).

References

1 L. F. Szczepura, L. M. Witham and K. J. Takeuchi, *Coord. Chem. Rev.*, 1998, **174**, 5.
2 A. G. Walden and A. J. M. Miller, *Chem. Sci.*, 2015, **6**, 2405.
3 A. Maleckis, J. W. Kampf and M. S. Sanford, *J. Am. Chem. Soc.*, 2013, **135**, 6618.
4 C. Moberg, *Angew. Chem. Int. Ed.*, 1998, **37**, 248.
5 H. R. Simmonds and D. S. Wright, *Chem. Commun.*, 2012, **48**, 8617.
6 F. García, A. D. Hopkins, R. A. Kowenicki, M. McPartlin, M. C. Rogers and D. S. Wright, *Organometallics*, 2004, **23**, 3884.
7 F. Reichart, M. Kischel and K. Zeckert, *Chemistry*, 2009, **15**, 10018.
8 K. Zeckert, S. Zahn and B. Kirchner, *Chem. Commun.*, 2010, **46**, 2638.
9 D. Morales, J. Pérez, L. Riera and D. Miguel, *Organometallics*, 2001, **20**, 4517.
10 I. Schrader, K. Zeckert and S. Zahn, *Angew. Chem. Int. Ed.*, 2014, **53**, 13698.
11 K. Zeckert, *Organometallics*, 2013, **32**, 1387.
12 R. Garcia-Rodriguez and D. S. Wright, *Dalton Trans.*, 2014, **43**, 14529.
13 C. Cui, R. A. Lalancette and F. Jaekle, *Chem. Commun.*, 2012, **48**, 6930.
14 R. Garcia-Rodriguez, T. H. Bullock, M. McPartlin and D. S. Wright, *Dalton Trans*, 2014, **43**, 14045.
15 C. S. Alvarez, F. Garcia, S. M. Humphrey, A. D. Hopkins, R. A. Kowenicki, M. McPartlin, R. A. Layfield, R. Raja, M. C. Rogers, A. D. Woods and D. S. Wright, *Chem. Commun.*, 2005, 198.
16 R. García-Rodríguez, H. R. Simmonds and D. S. Wright, *Organometallics*, 2014, **33**, 7113.

17 F. Garcia, A. D. Hopkins, R. A. Kowenicki, M. McPartlin, M. C. Rogers, J. S. Silvia and D. S. Wright, *Organometallics*, 2006, **25**, 2561
18 R. Garcia-Rodriguez and D. S. Wright, *Chem. Eur. J.*, 2015, **21**, 14949.
19 R. Garcia-Rodriguez, S. Hanf, A. D. Bond and D. S. Wright, *Chem. Commun.*, 2017, **53**, 1225.
20 a) A. N. W. Kuda-Wedagedara, C. Wang, M. J. Allen and P. D. Martin, *J Am. Chem. Soc.*, 2015, **137**, 4960; b) R. P. Kelly, T. D. M. Bell, R. P. Cox, D. P. Daniels, G. B. Deacon, F. Jaroschik, P. C. Junk, X. F. Le Goff, G. Lemercier, A. Martinez, J. Wang and D. Werner, *Organometallics*, 2015, **34**, 5624.
21 a) I. V. Basalov, O. S. Yurova, A. V. Cherkasov, G. K. Fukin and A. A. Trifonov, *Inorg. Chem. 2016*, **55**, 1236; b) F. T. Edelmann, *Chem. Soc. Rev. 2012*, **41**, 7657.
22 *Lehrbuch der anorganischen Chemie*, M. Krieger-Hauwede, A. F. Holleman, N. Wiberg, 102 ed., Berlin, 2007.
23 T. D. Tilley, R. A. Andersen, B. Spencer, H. Ruben, A. Zalkin and D. H. Templeton, *Inorg. Chem.*, 1980, **19**, 2999.
24 *Synthetic Methods of Organometallic and Inorganic Chemistry. Vol. 6. Lanthanides and Actinides*, ed. F. T. Edelmann, George Thieme Verlag, Stuttgart, 1997.
25 K. Zeckert, J. Griebel, R. Kirmse, M. Weiss and R. Denecke, *Chem. Eur. J.*, 2013, **19**, 7718.
26 For example, see X. W. Zhang, G, H, Maunder, X. Geissmann, R. McDonald, M. J. Ferguson, A. D. Bond, R. D. Rogers, A. Sella and J. Takats, *Dalton Trans*., 2011, **40**, 195, and references therein.
27 *Inorganic Chemistry: Principles of Structure and Reactivity*, J. Huyee, E. A. Keiter, R. L. Keiter, Harper Collins, 4th Ed., 1993, pp. 290.
28 T. Kottke and D. Stalke, *J. Appl. Crystallogr*. 1993, **26**, 615.

